Physicochem. Probl. Miner. Process., 55(3), 2019, 597-604

http://www.journalssystem.com/ppmp

Physicochemical Problems of Mineral Processing

ISSN 1643-1049

Received May 7, 2018; reviewed; accepted September 7, 2018

Application of superconducting magnetic separation to an artificial mixture of chalcopyrite and molybdenite

Daokui Li, Jue Kou, Chunbao Sun, Baoqiang Yu, Chao Wang

School of Civil and Environmental Engineering, University of Science and Technology Beijing, Beijing 100083, China

Corresponding author: koujue@ustb.edu.cn (Jue Kou)

Abstract: Superconducting magnetic separation of chalcopyrite and molybdenite was studied, along with the effects of the magnetic flux density, slurry concentration, and pulsation amplitude on the separation. According to the force equilibrium model of magnetic particles that accumulated on magnetic matrices during the superconducting magnetic separation, the saturated buildup of magnetic particles was calculated. The saturated buildup of magnetic particles was an approximate fan ring and had a positive correlation with the background magnetic flux density. Superconducting magnetic separation tests results showed that a Mo concentrate with a Mo grade of 31.86% and recovery of 87.24% and a Cu concentrate with a Cu grade of 30.57% and recovery of 94.76% could be obtained. This verified the feasibility of separating mixed Cu and Mo minerals via superconducting magnetic separation.

Keywords: superconducting magnetic separation, chalcopyrite and molybdenite separation, magnetic matrices, buildup behavior

1. Introduction

Mo is a very important strategic material that is widely used in metallurgy, electronics, automobile manufacturing, aviation, and the nuclear industry (Xu J. et al., 2005). Mo resources are mostly derived from porphyry copper molybdenum deposits and are often closely associated with chalcopyrite (Dong Y., 2017). In industrial production, flotation is commonly used to separate chalcopyrite and Mo. However, the current separation process is complicated and requires a large dosage of the inhibitor Na_2S, which leads to high operating costs and environmental issues (Meng Q. et al., 2014).

Superconducting magnetic separation using a superconducting magnet as a magnetic system has the advantages of a high magnetic flux density, a large processing capacity, low energy consumption, and low operating costs (He L., 2013). The commonly used superconducting materials are Nb-Zr alloys, Nb-Ti alloys, and Nb_3Sn compounds. Because its resistance is nearly zero, the superconducting magnet consumes little energy. By using superconducting welding closure technology, the current can be locked in the coil to form a continuous current; thus, a constant strong magnetic field with high stability, good uniformity, and strong controllability can be obtained (Sun Z. et al., 2012). Superconducting magnetic separation is mainly applied in the fields of kaolin clay beneficiation, coal desulfurization, and sewage treatment (Ohara, T. et al., 2001). For example, the Yankuang group of Guangxi province, China, achieved good results, with an average Fe removal rate of 22.9% and an average increase of 2.06% in the natural whiteness by using superconducting magnetic separation technology to remove impurities from kaolin (Mo C. et al., 2009). At present, superconducting magnetic separation technology can produce a magnetic flux density of 4–8 T. Therefore, extremely weak magnetic minerals that cannot be separated by normal magnetic separation can be separated by superconducting magnetic separation.

Studies (Liu L. et al., 2017) have shown that chalcopyrite is a paramagnetic material with average magnetic susceptibility of 67.53×10^{-9} m^3/kg. Molybdenite is a diamagnetic material with average magnetic susceptibility of -0.098×10^{-9} m^3/kg. Therefore, by using the magnetic difference, it is theoretically possible to separate chalcopyrite and molybdenite via the superconducting magnetic

DOI: 10.5277/ppmp18171

separation method. In this study, the superconducting magnetic separation of chalcopyrite and molybdenite, along with the effects of the magnetic flux density, slurry concentration, and pulsation amplitude on the separation, is examined for the first time. The buildup of magnetic particles in the magnetic matrices is analyzed, providing a new method and direction for the separation of mixed Cu-Mo minerals, as well as a new method for the separation and recovery of non-ferrous metal minerals.

2. Materials and methods

2.1. Materials

Pure chalcopyrite and molybdenite minerals from China Tibet Huatailong Mining Co., Ltd. were used to explore the possibility of Cu-Mo superconducting magnetic separation. The purity of the chalcopyrite and molybdenite was 94.42% and 91.80%, respectively. The impurities were small amounts of quartz, feldspar, and pyrite. In the test, the pure minerals were crushed to -5 mm and then ground to -0.074 mm using a ceramic ball mill. According to the contents of Cu and Mo in mixed concentrate from most Cu mines, pure chalcopyrite and molybdenite minerals at a mass ratio of 7:1 were uniformly blended as test samples. The particle size, grade, and purity of the test samples are listed in Table 1.

Table 1. Properties of test sample

Item \ Mineral samples	Chalcopyrite	Molybdenite
-0.074 mm /%	100	84.5
Cu /%	32.85	/
Mo /%	/	55.08
purity /%	94.42	91.8

2.2. Methods

The superconducting magnetic separator D102 with a reciprocating sorting structure produced by Jiangsu Jingkai Zhongke Superconducting High-tech Co., Ltd. Was used in the test. The magnetic flux density ranged from 0 to 5 T, and the pulsation frequency was adjustable from 0 to 50 Hz. The inside diameter of the separation chamber was 102 mm. The superconducting magnetic separation system, as shown in Fig. 1, mainly consisted of a superconducting coil, a separation chamber, and magnetic matrices. The superconducting coil was immersed in liquid He, and the resistance was close to zero. A high-intensity magnetic field was generated by direct current excitation, so that the magnetic matrices generated a high-gradient magnetic field, and weak magnetic particles were held onto the surface of the magnetic matrices by the magnetic force. Condition tests, including the magnetic flux density, slurry concentration, and pulsation amplitude, were conducted in the superconducting magnetic separator D102. The product index can be evaluated according to the grade and recovery. The grade of Cu was determined via atomic absorption spectrometry, and the grade of Mo was determined via thiocyanate spectrophotometry. The recovery is given by Eq. (1):

$$\text{Recovery } (\varepsilon), \% = \gamma(\beta/\alpha) \times 100 \tag{1}$$

where γ is the yield (γ = amount of concentrate, g/amount of the raw sample, g), β is the grade of the concentrate, and α is the grade of the raw sample.

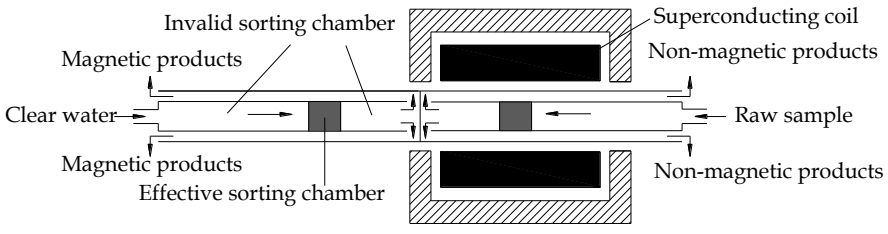

Fig. 1. Equipment working principle

2.3. Pure mineral magnetic hysteresis loop test

The magnetic hysteresis loop of pure chalcopyrite was measured, and the results are shown in Fig. 2. We observe that when the magnetic flux density increased from 0 to 1 T, the mass magnetic moment of the chalcopyrite sharply increased. The chalcopyrite mass magnetic moment slowly and linearly increased when the magnetic flux density increased from 1 to 5 T.

The magnetic susceptibility of chalcopyrite can be calculated using Eq. (2).

$$\chi = M/(H \times m) \tag{2}$$

where H is the magnetic flux density, M is the ore particle magnetic moment, and m is the material mass ($1\ A/m = 4\pi \times 10^{-3}$ Oe, $1\ A \cdot m^2 = 10^3$ emu).

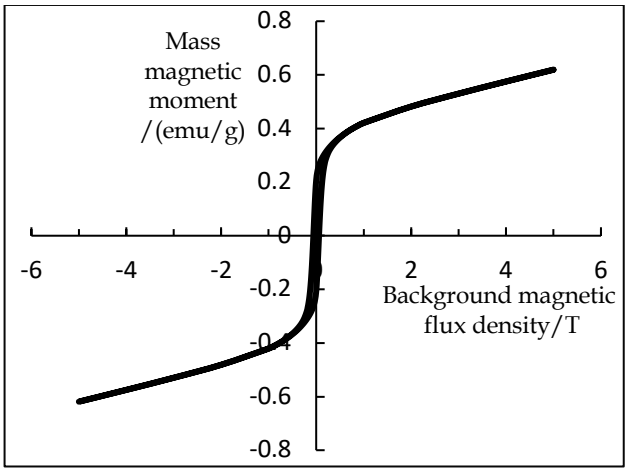

Fig. 2. Magnetic hysteresis loop of chalcopyrite

3. Results and discussion

3.1. Effect of magnetic flux density on Cu and Mo separation

Superconducting magnetic separation tests with magnetic flux densities of 1.5, 3.5, and 5 T were conducted under the following conditions: a slurry mass concentration of 10%, a flow rate of 1 cm/s, magnetic matrices of No. 5 steel wool, a pulsation impulse of 250 rpm, and a pulsation amplitude of 15 mm. The test results are shown in Table 2.

Table 2. Experimental results for the superconductivity magnetic separation of Cu and Mo with different magnetic flux densities

Magnetic flux density /T	Product name	Yield /%	Grade /%		Recovery /%	
			Mo	Cu	Mo	Cu
1.5	Cu concentrate	72.99	1.49	29.86	13.30	82.77
	Mo concentrate	27.01	26.24	16.8	86.70	17.23
	Raw sample	100.00	8.18	26.33	100.00	100.00
3.5	Cu concentrate	78.90	2.03	30.64	19.05	91.47
	Mo concentrate	21.10	32.24	10.69	80.95	8.53
	Raw sample	100.00	8.41	26.43	100.00	100.00
5	Cu concentrate	87.29	2.78	30.18	29.88	99.39
	Mo concentrate	12.71	44.80	1.27	70.12	0.61
	Raw sample	100.00	8.12	26.5	100.00	100.00

The experimental results show that with the increasing magnetic flux density, the grade and recovery of Mo from the Cu concentrate increased. The grade of Mo from the Mo concentrate gradually increased, but the recovery gradually decreased. Mo concentrate with a Mo grade of 44.80% and recovery of 70.12% was obtained when the magnetic flux density was 5 T. A higher magnetic flux

density led to higher Mo recovery from the Cu concentrate but lower Mo recovery from the Mo concentrate.

3.2. Effect of slurry concentration on Cu and Mo separation

Superconducting magnetic separation tests with different slurry concentrations of 1%, 5%, and 10% were conducted using magnetic matrices of No. 5 steel wool, a flow rate of 1 cm/s, a magnetic flux density of 5 T, a pulsation impulse of 250 rpm, and a pulsation amplitude of 15 mm. The test results are shown in Table 3.

Table 3. Experimental results for the superconductivity magnetic separation of Cu and Mo with different slurry concentrations

Slurry concentration /%	Product name	Yield /%	Grade /%		Recovery /%	
			Mo	Cu	Mo	Cu
1	Cu concentrate	87.29	2.78	30.18	29.88	99.39
	Mo concentrate	12.71	44.80	1.27	70.12	0.61
	Raw sample	100.00	8.12	26.50	100.00	100.00
5	Cu concentrate	88.23	2.94	30.18	32.50	98.97
	Mo concentrate	11.77	45.76	2.37	67.50	1.03
	Raw sample	100.00	7.98	26.90	100.00	100.00
10	Cu concentrate	89.08	2.84	28.81	31.85	98.58
	Mo concentrate	10.92	49.56	3.39	68.15	1.42
	Raw sample	100.00	7.94	26.03	100.00	100.00

The test results show that with the increase of the slurry concentration, the Mo grade in the Mo concentrate increased, while the recovery decreased. At a slurry concentration of 10%, the Mo grade and recovery were 49.56% and 68.15%, respectively. Owing to the small size of the ore particles, the large surface energy, and the effect of the unsaturated bond energy, the ore particles were mutually agglomerated, the slurry was not easily dispersed, and the chalcopyrite contained molybdenite. When the particles were in the magnetic field, ore particle magnetization and magnetic agglomeration occurred. A higher slurry concentration led to a higher likelihood of magnetic agglomeration and lower Mo recovery from the Mo concentrate.

3.3. Effect of pulsation amplitude on Cu and Mo separation

Superconducting magnetic separation at different pulsation amplitudes of 10, 15, and 20 mm was tested under the following conditions: a slurry mass concentration of 10%, a flow rate of 1 cm/s, a magnetic flux density of 5 T, and a pulsation impulse of 250 rpm. The test results are shown in Table 4.

Table 4. Experimental results for the superconductivity magnetic separation of Cu and Mo with different pulsation amplitudes

Pulsation amplitude /mm	Product name	Yield /%	Grade /%		Recovery /%	
			Mo	Cu	Mo	Cu
10	Cu concentrate	80.24	3.35	28.31	34.52	91.57
	Mo concentrate	19.76	29.56	12.43	65.77	6.86
	Raw sample	100.00	8.25	25.23	100.00	100.00
15	Cu concentrate	79.77	2.29	29.45	21.61	94.02
	Mo concentrate	20.23	32.74	7.38	78.39	5.98
	Raw sample	100.00	8.45	24.98	100.00	100.00
20	Cu concentrate	78.19	1.30	30.57	12.76	94.76
	Mo concentrate	21.81	31.86	6.06	87.24	5.24
	Raw sample	100.00	7.966	25.22	100.00	100.00

The test results show that the grade and recovery of Cu from the Cu concentrate increased gradually with the increase of the pulsation amplitude from 10 to 25 mm. The Mo recovery from the Mo concentrate increased from 65.77% to 87.24%. A good separation index was obtained at a pulsation amplitude of 15 mm. Under the action of a pulsating water flow, the particles in the sorting chamber were kept in a loose state. Thus, the chalcopyrite particles were more easily captured by the magnetic matrices, and the molybdenite particles passed through the magnetic matrices as quickly as possible.

4. Mechanism analysis and discussion

4.1. Force analyses

Superconducting magnetic separation is usually performed in aqueous media. The forces acting on the particles include gravity, buoyancy, fluid drag, Brownian forces, inertial forces, and magnetic forces (Lim et al., 2014). As particle size decreases, some forces can be neglected, as they are weak compared with other dominant forces (Moeser et al., 2004; Cafer T. Yavuz et al., 2006). In this study, the main forces were the magnetic force and fluid drag. Fig. 3 shows all the forces acting on the particles. Assumptions were made, e.g., that the particle is spherical and is temporarily stationary on the surface of the matrices. The magnetic force acting on the particles around the matrices can be derived in terms of the polar coordinates (Watson, 1973; Luborsky and Drummond, 1975).

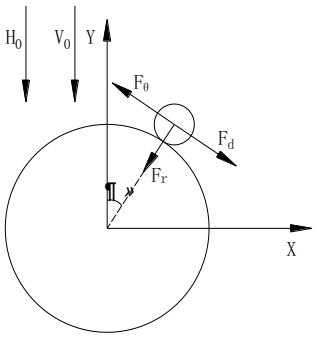

Fig. 3. Force components acting on the particle at rest on the matrix

For a field-dependent susceptibility mineral particle, the radial and tangential components of the magnetic force are given by Eqs. (3) and (4), respectively.

$$F_r = -\frac{8}{3}\pi R^3(k_\infty H_0 + fM_0)H_0\frac{A_p d^2}{r^3}\left(\cos 2\theta + \frac{A_p d^2}{r^2}\right) \quad (3)$$

$$F_\theta = -\frac{8}{3}\pi R^3(k_\infty H_0 + fM_0)H_0\frac{A_p d^2}{r^3}\sin 2\theta \quad (4)$$

Here, R is the radius of the paramagnetic particle, k_∞ is the magnetic susceptibility in an infinite magnetic field, M_0 is the spontaneous magnetization, H_0 is the applied magnetic field, d is the radius of the matrix cross section, r is the distance between the particle and the matrix axis, and θ is the angle from the front stagnant point. The field factor f is given as follows:

$$f = \frac{1}{2\left(1+\frac{2A_p d^2}{r^2}\cos 2\theta+\frac{d^4 A_p^2}{r^4}\right)^{1/2}} \quad (5)$$

where A_p is the perturbation item for the cylinder matrix and is given as:

$$A_p = \frac{2\pi M_w}{H_0} \quad (6)$$

Here, M_w is the matrix magnetization. The fluid drag force is only in the tangential direction and is calculated using the shear stress at the bottom of the boundary layer, which was derived from the Blasius solutions to the boundary layer equations. Considering the expansion to θ^{11}, the fluid drag force can be given as follows (Schlichting, 1968):

$$F_d = \frac{\pi^2 R^2}{4}\rho_f V_0^{3/2}\left(\frac{\nu_f}{r}\right)^{1/2}(6.973\theta - 2.732\theta^3 + 0.292\theta^5 - 0.0183\theta^7 + 0.000042\theta^9 + 0.000115\theta^{11}) \quad (7)$$

where ρ_f is the fluid density, V_0 is the fluid initial velocity, and ν_f is the fluid kinematic viscosity ($\nu_f = \eta/\rho_f$).

4.2. Buildup of magnetic particles on matrix

The accumulation of magnetic particles on the magnetic matrices is considered to occur layer-by-layer. Thus, the resultant force of the magnetic particles must be calculated layer-by-layer. For the first layer, r = d + R; for the second layer, r = d + R + $\sqrt{R}$; for the third layer, r = d + R + 3$\sqrt{R}$; and so on (Zheng X. et al., 2014). For each layer, the θ value is calculated when the radial and tangential forces are equal to 0, and the smaller one is selected. A series of θ values and the corresponding r values can be calculated to obtain the cumulative profile of the magnetic particles on the magnetic matrices. Then, the accumulation status and saturation of the magnetic particles on the magnetic matrices can be obtained, and the accumulation behavior of the magnetic particles on the magnetic matrices can be analyzed.

In superconducting magnetic separation, the perturbation term A_p is approximately 0.44, 0.28, 0.16, and 0.09 when the magnetic induction is 2, 3, 4, and 5 T, respectively. Chalcopyrite was chosen as the representative field-dependent susceptibility mineral, with k_∞ = 0.0053, M_0 = 0.0103 T, and a density of ρ_f = 4,260 kg/m^3 (Nesset and Finch, 1980). The fluid had a density of ρ_f = 1,000 kg/m^3 and a viscosity of η = 1 mPa · s.

$$V_s/V_d = \frac{(R_s^2 - d^2)\varphi}{2\pi d^2} \tag{8}$$

The size of the matrix has a significant effect on the buildup of magnetic particles. Assume that V_d is the volume of magnetic matrices and V_s is the volume of magnetic particles accumulated on the magnetic matrices. For a superconducting magnetic separation system with the same matrix filling rate, the total amount of particles that accumulate on the magnetic matrices is only related to V_s/V_d. Therefore, V_s/V_d can be used to analyze the influence of the magnetic matrix size on the buildup of magnetic particles. Assuming that the magnetic particles accumulate in the axial direction of the matrix, the cumulative volume of magnetic particles is the product of the cross-sectional area of the magnetic particles and the axial length of the matrix. It can be seen that the value of V_s/V_d is equal to the ratio of the cross-sectional area of cumulative magnetic particles to the cross-sectional area of the magnetic matrices, and the buildup of magnetic particles is an approximate fan ring. Fig. 4 shows a schematic of an approximate fan ring of the saturated buildup of magnetic particles. The red curve in the figure represents the saturated buildup of magnetic particles, and the green curve represents the imaginary approximate sector. The normalized buildup of magnetic particles V_s/V_d can be calculated using Eq. (8).

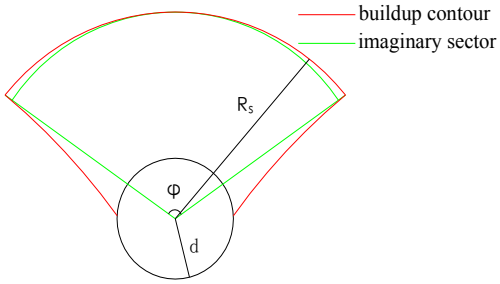

Fig. 4 Schematic of the imaginary sector of the buildup contour

The effect of the magnetic flux density on the saturated buildup of particles is shown in Fig. 5. The magnetic flux density influences the magnetization state and susceptibility of the magnetic particles, thereby affecting the buildup of magnetic particles. As shown in Fig. 5, the saturated buildup of magnetic particles increases with the magnetic flux density. A higher magnetic flux density is favorable for the buildup of magnetic particles. However, when the background magnetic flux density exceeds a certain value, the recovery of magnetic minerals remains unchanged or even decreases (Svoboda, 1994). This is because when the magnetization of the magnetic matrices is saturated, the magnetic-field gradient produced by the magnetic matrices does not change, and non-selective magnetic flocculation may cause non-magnetic particle inclusion under a high magnetic field.

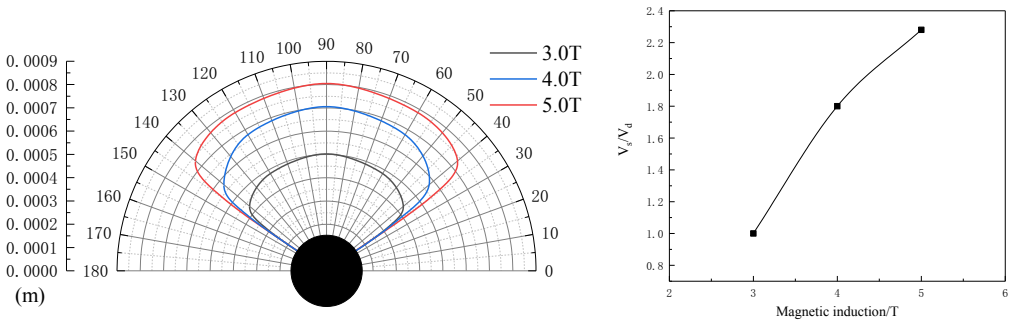

（a） (b)

Fig. 5. Effect of the magnetic flux density on the saturated buildup of particles (particle radius of R = 10 μm, matrix radius of d = 0.1 mm, and fluid velocity of V_0 = 0.01 m/s).

5. Conclusions

The saturated buildup of magnetic particles on magnetic matrices reflects the maximum buildup of magnetic particles on magnetic matrices. According to the force balance model of magnetic particles that accumulate on magnetic matrices during superconducting magnetic separation, the saturated buildup of magnetic particles on magnetic matrices at different magnetic flux densities was calculated. For the same size of magnetic matrices, the saturated buildup of magnetic particles increased with the background magnetic flux density. The results of superconducting magnetic separation tests on mixed Cu and Mo minerals show that Mo concentrate with a Mo grade of 31.86% and recovery of 87.24%, as well as Cu concentrate with a Cu grade of 30.57% and recovery of 94.76%, can be obtained by increasing the magnetic flux density, selecting the appropriate magnetic matrices, and using a pulsation device. The feasibility of separating mixed Cu and Mo minerals via superconducting magnetic separation was verified theoretically and experimentally, providing a new method for the separation of Cu and Mo minerals.

References

DONG Y.,2017. *Experimental study on flotation and separation of a low-grade copper-molybdenum ore.* China Molybdenum Industry, 42(4), 10-16.

HE L., 2013. *Application of superconducting magnetic separation.* Cryogenics and Superconductivity, 753-755, 114-118.

LIM, J.K., YEAP, S.P., LOW, S.C., 2014. *Challenges associated to magnetic separation of nanomaterials at low field gradient.* Sep. Purif. Technol. 123, 171–174.

LI W., 2015. *Study on magnetic induction properties and magnetic separation behaviors of magnetic matrices.* PhD thesis, Northeastern University.

LIU L., LV L., MA Y., LI W., WANG S., 2017. *Study on superconducting magnetic separation dealing with fine molybdenum concentrate containing copper.* Conservation and Utilization of Mineral Resources, (1), 55-58.

MOESER, G.D., ROACH, K.A., GREEN, W.H., HATTON, T.A., 2004. *High-gradient magnetic separation of coated magnetic nanoparticles.* AIChE J. 50 (11), 2835–2848.

MENG Q, CUI Y Q, TONG X, ZHOU HJ, WANG K., 2014. *Research status of copper-molybdenum separation.* Mining and Metallurgy, 23(2), 19-22.

MO C., WEI X., 2009. *Research on the application of superconducting magnetic separation of Beihai kaolin.* Nonmetallic Mines, 32(1), 9-10.

NESSET, J.E., FINCH, J.A., 1980. *A loading equation for high gradient magnetic separators and application in identifying the fine size limit of recovery.* In: Somasundaran, P. (Ed.), Fine Particles Processing. AIME, New York, 1217–1241.

OHARA, T., KUMAKURA, H., WADA, H.,2001. *Magnetic separation using superconducting magnets.* Physica C Superconductivity and Its Applications, 357(8), 1272-1280.

SCHLICHTING, H., 1968. *Boundary-Layer Theory.* Mc Graw-Hill, New York, 154.

SVOBODA, J., 1994. *The effect of magnetic field strength on the efficiency of magnetic separation.* Miner. Eng. 7 (5–6), 747–757.

SUN Z., ZHU Z., WANG M., LI P., ZHANG Y., 2012. *Development of superconducting magnetic separation equipment.* Review and Prospect of China's Selection Technology, 599-604.

WATSON, J.H.P., 1973. *Magnetic filtration.* J. Appl. Phys. 44 (9), 4209–4213.

WATSON, J.H.P., 1975. *Theory of capture of particles in magnetic high-intensity filters.* IEEE Trans. Magn. 11 (5), 1597–1599.

XU J., YANG L., WANG J., 2005. *Study on the utilization of china molybdenum resources and sustainable development.* China Molybdenum Industry, 29(4), 3-9.

YAVUZ CT, MAYO JT, YU WW, PRAKASH A, FALKNER JC, YEAN S, CONG L, SHIPLEY HJ, KAN A, TOMSON M, NATELSON D, COLVIN VL., 2006. *Low-field magnetic separation of monodisperse Fe_3O_4 nanocrystals.* Science, 314 (5801), 964-967.

ZHENG X., WANG Y., LU D., 2015. *A realistic description of influence of the magnetic field strength on high gradient magnetic separation.* Minerals Engineering, 79, 94-101.